ON THE CROSS-FIELD DIFFUSION OF GALACTIC COSMIC RAYS INTO AN ICME

K. MUNAKATA*,‖, S. YASUE*, C. KATO*, J. KOTA†, M. TOKUMARU‡, M. KOJIMA‡, A. A. DARWISH§, T. KUWABARA¶ and J. W. BIEBER¶

*Department of Physics, Shinshu University
Asahi 3-1-1, Matsumoto, Nagano 390-8621, Japan

†Lunar and Planetary Laboratory, University of Arizona
Tucson, AZ, USA

‡Solar Terrestrial Environmental Laboratory, Nagoya University
Nagoya, Japan

§Physics Department, Faculty of Science, Alexandria University
Alexandria, Egypt

¶Bartol Research Institute and Department of Physics and Astronomy
University of Delaware, Newark, Delaware, USA
‖kmuna00@gipac.shinshu-u.ac.jp

We develop a numerical model of the cross-field diffusion of galactic cosmic rays into an interplanetary coronal mass ejection (ICME), on the assumption that the local part of the ICME is an expanding straight cylinder. It is found that the spatial distribution of cosmic ray density in the cylinder rapidly reaches a stationary state due to the balance between inward diffusion and adiabatic cooling in the expanding cylinder. By fitting the model to the Halloween ICME event observed with the network of muon detectors in October 2003, we evaluate the magnitude of the cross-field diffusion coefficient to be 1.7×10^{21} cm^2/s at ~ 50 GeV.

1. Introduction

When the Interplanetary counterpart of a Coronal Mass Ejection (ICME) accompanied by a strong shock travels through interplanetary space, it often forms a depleted region of Galactic cosmic rays behind the shock and within the ICME, changing dramatically the pre-existing spatial distribution of cosmic rays. When Earth enters the depleted region, ground-based cosmic ray detectors record a Forbush Decrease.[1] This change in the spatial distribution can be observed by cosmic ray (CR) detectors at Earth as a dynamic variation of the directional anisotropy of CR intensity (or the CR streaming), since the CR anisotropy corrected for convection by the solar wind is solely due to spatial diffusion and drift fluxes that are

proportional to the spatial gradient of the cosmic ray density (the isotropic component of the intensity) in local space. Bieber and Evenson[2] reported such strong enhancements of the anisotropy observed by a network of seven neutron monitors and concluded that "$\mathbf{B} \times \nabla n$" drift is a primary source of ICME-related anisotropies. They demonstrated for the first time that the evolution of CR density and density gradients is closely linked to magnetic properties of the ejecta, and provides information on the structure and orientation of the ICME as it approaches and passes Earth.[3] Hofer and Flückiger[4] also analyzed the anisotropy observed by neutron monitors during a large Forbush Decrease in March 1991 and demonstrated the potential capability of CR observations for providing information on complex transient structures in the near-Earth interplanetary medium.

Kuwabara *et al.*[5,6] modeled the CR depleted region in the Halloween ICME observed by the muon detector network on October 29, 2003, by a straight cylinder and deduced the three-dimensional (3D) geometry of the cylinder. They also compared the geometry derived from cosmic rays with that derived from *in situ* interplanetary magnetic field (IMF) observations using an expanding Magnetic Flux Rope (MFR) model, and demonstrated that these two geometries based on independent observations are in a reasonable agreement. Cane *et al.*[7] presented for the first time a quantitative study of the cross-field diffusion of CRs into an ICME and derived the density distribution in the ICME. Their model, however, assumed a stationary ICME with a constant radius ignoring the adiabatic cooling of CRs that occurs in an expanding ICME. Such a model is not applicable to the Halloween ICME, in which the *in situ* observations of the IMF clearly indicate expansion.[5,6]

In the present paper, we develop a numerical model for the cross-field diffusion of CRs into an expanding ICME, taking account of the adiabatic cooling effect due to expansion. In Sec. 2, we first derive the CR density distribution in the ICME based on the transport equation of CRs. In Sec. 3, we apply the model to the Halloween ICME event observed by the muon detector network and deduce the magnitude of the cross-field diffusion coefficient appropriate to the observation. Due to the closed field geometry, CRs can penetrate in the MFR only through cross-field diffusion. This provides us with a unique opportunity to precisely evaluate the cross-field diffusion coefficient, which is one of the most difficult physical parameters to estimate from observations.

We note that MFRs are a subset of ICME with a special magnetic structure (see Ref. 5 and references therein for details). Our Forbush decrease

model derived in Sec. 2, does not explicitly assume MFR structure, and thus should apply generally to any ICME that can be modeled as an expanding cylinder. However, our method used to analyze the Halloween event in Sec. 3, employs parameters derived from a MFR analysis of the ICME, and thus can only be applied to the MFR subset of ICME.

2. Model and Numerical Solutions

2.1. *Transport equation*

The axisymmetric distribution of the CR density in a cylinder is governed by the following transport equation for the cross-field diffusion of CRs into the ICME, which is assumed to be a cylinder in this paper.

$$\frac{\partial f}{\partial t} = \frac{\kappa_\perp}{r}\frac{\partial}{\partial r}\left(r\frac{\partial f}{\partial r}\right) - V\frac{\partial f}{\partial r} + \frac{1}{3r}\frac{\partial}{\partial r}(rV)\frac{\partial f}{\partial \ln p}\,, \tag{1}$$

where $f(r, p, t)$ is the omnidirectional phase space density of CRs with momentum p at a radial distance r from the ICME (cylinder) axis and time t and V is the radial expansion velocity of the ICME. The first and second terms on the right hand side denote respectively the cross-field diffusion and the convection in the expanding plasma, while the third term denotes the adiabatic cooling due to expansion.

We rewrite (1) for $f(x, p, s) = f(r, p, t)$ by replacing r and t, respectively with dimensionless quantities x and s, defined as,

$$x = \frac{r}{R(t)} \quad \text{and} \quad s = \log\left(\frac{t}{t_c}\right), \tag{2}$$

with $R(t)$ denoting the radius of the ICME envelope at time t and t_c denoting an arbitrary reference time. We assume self-similar expansion of the ICME[3] with radius $R(t)$ and expansion velocity V defined as

$$V(r, t) = \frac{r}{t}\,, \tag{3}$$

$$R(t) = \frac{R_c t}{t_c}\,, \tag{4}$$

with R_c denoting $R(t)$ at $t = t_c$. In the following analyses, we define $t = t_c$ as the time of Earth's first contact with the ICME envelope. We also assume $\kappa_\perp$ independent of x, but proportional to the radius of the ICME envelope. This seems to be a reasonable assumption, since the self-similar expansion

of the ICME will increase the diffusion mean-free-path as well. We assume $\kappa_\perp$ can be expressed as

$$\kappa_\perp = \kappa_0 V_c R(t)\,, \tag{5}$$

where κ_0 is a dimensionless parameter denoting the degree of the cross-field diffusion, and V_c the expansion velocity of the ICME envelope at t_c. We finally assume a single power momentum spectrum for f, as

$$f(x,p,s) = p^{-(2+\gamma)} F(x,s)\,, \tag{6}$$

with the spectral index γ set equal to 2.7, as appropriate for high-energy Galactic cosmic rays. We thus obtain the equation to be solved numerically, as

$$\frac{\partial F}{\partial s} = \kappa_0 \left(\frac{\partial^2 F}{\partial x^2} + \frac{1}{x}\frac{\partial F}{\partial x} \right) - \frac{2(2+\gamma)}{3} F\,. \tag{7}$$

Note that the convection term in (1) does not appear in this equation.

2.2. *Numerical solutions*

We solve (7) numerically with an initial condition that the CR density is zero inside and uniform outside the ICME (i.e., starting from an "empty cylinder"). More practically, we set $F = 0$ for $x < 1.0$ and $F = 1$ for $x \geq 1.0$ as the initial condition at $s = -4.605\,(t = 0.01 \times t_c)$. Figure 1 shows numerical solutions of (7). As seen in this figure, the spatial distribution $F(x)$ for $\kappa_0 > 1$ rapidly reaches an equilibrium due to the balance between inward diffusion (causing an increase of F) and adiabatic cooling (causing a decrease of F) within $s < -2.303$ ($t < 0.1 \times t_c$). Since we define $s = 0.0$ ($t = t_c$) as the time of Earth's first contact with the ICME surface, Fig. 1 implies that F is already stationary when the ICME arrives at Earth. The magnitude of the maximum density depression $(1 - F(0,\infty))$ in this stationary distribution is shown as a function of κ_0 in Fig. 2(a). As the maximum density depression in Forbush Decreases observed by muon detectors is typically $1 \sim 10\%$ ($0.01 \sim 0.1$), this figure implies that the magnitude of κ_0 appropriate to the observation should be 10–50.

The stationary distribution $F^{\rm stat}(x)$ is given by (7) with the left hand side set equal to zero, as

$$\kappa_0 \left(\frac{\partial^2 F^{\rm stat}}{\partial x^2} + \frac{1}{x}\frac{\partial F^{\rm stat}}{\partial x} \right) = \frac{2(2+\gamma)}{3} F^{\rm stat}\,. \tag{8}$$

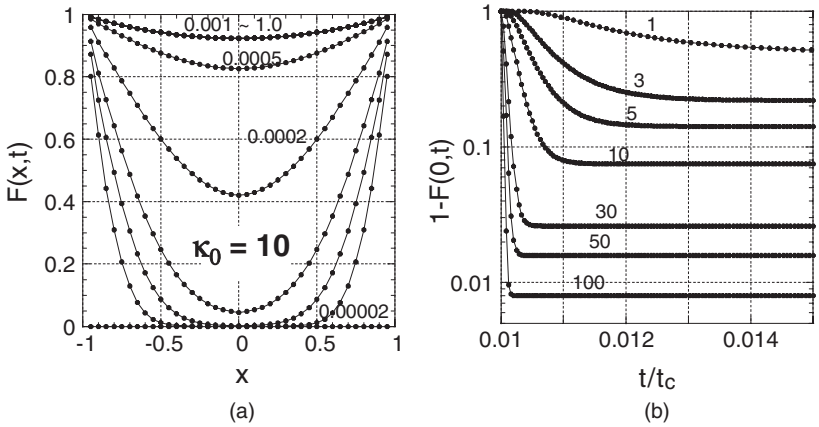

Fig. 1. Numerical solutions of (7). (a) The density distributions are plotted as a function of normalized radial distance x from the ICME axis at different times. Each number attached to the curve indicates the normalized time after t_c ($t/t_c - 1.0$). The numerical distribution for $x \geq 0$ is repeated for $x < 0$ to clarify the physical distribution. (b) The temporal evolution of the magnitude of maximum density depression at $x = 0$ on the ICME axis. Each number attached to the curve indicates the value of κ_0.

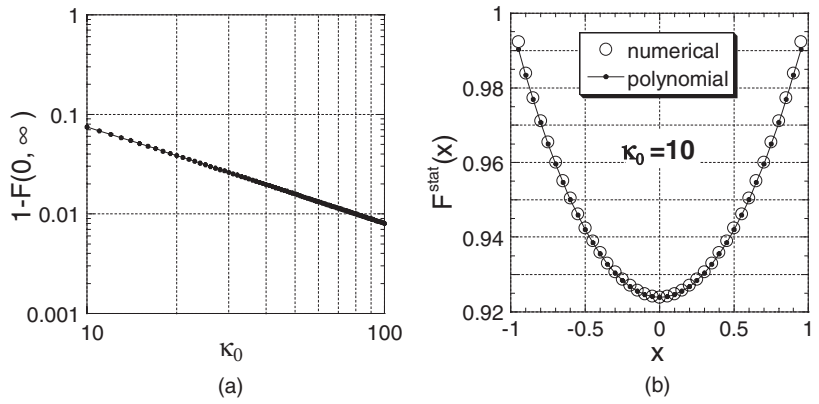

Fig. 2. Stationary solutions of (7). (a) The magnitude of maximum density depression in numerical solution is plotted as a function of κ_0. (b) The stationary distribution for $\kappa_0 = 10$ is plotted in the same manner as Fig. 1(a). The full circles connected by a line display the numerical solution, while the open circles represent the polynomial solution (see text).

The solution is a Bessel function which we approximate with a polynomial:

$$F^{\rm stat}(x) = \sum_{n=0}^{\infty} a_n x^n \,, \tag{9}$$

then we obtain,

$$a_n = \left(\frac{\Gamma}{n^2}\right) a_{n-2} \quad \text{for } n = 2, 4, 6, \ldots \tag{10}$$

and

$$a_n = 0 \quad \text{for } n = 1, 3, 5, \ldots \tag{11}$$

where

$$\Gamma = \frac{2(2+\gamma)}{3\kappa_0} \,. \tag{12}$$

Figure 2(b) shows this polynomial solution for $\kappa_0 = 10$ and $n \leq 6$, together with $F(x, \infty)$ obtained by solving (7) numerically. It is seen that the numerical solution is well reproduced by the polynomial expression with $n \leq 6$. In Sec. 3, we will use this expression for best-fitting to the observed data.

3. Best-Fitting to the Halloween ICME Event

In this section, we derive the magnitude of κ_0 appropriate to the Halloween ICME event observed on October 29, 2003, by best-fitting the model in the previous section to the observed data. Although a substantial CR depression also commenced at the time of the passage of a strong shock ahead due to the modulation by the post-shock region, we restrict ourselves in modeling only the modulation in the ejecta behind the shock in this paper. A more complete model will be given elsewhere in the future.

Using the polynomial solution $F^{\rm stat}(x)$ in (9), we get the expected fractional density depression $I^{\rm exp}(t_i)$ and the fractional density gradient vector $\mathbf{g}_\perp^{\rm exp}(t_i)$ at time t_i, as

$$I^{\rm exp}(t_i) = a_0 \left\{ 1 + \frac{\Gamma}{4} x(t_i)^2 + \frac{\Gamma^2}{64} x(t_i)^4 + \cdots \right\}, \tag{13}$$

$$\mathbf{g}_\perp^{\rm exp}(t_i) = -\frac{a_0}{I^{\rm exp}(t_i)} \left\{ \frac{\Gamma}{2} x(t_i) + \frac{\Gamma^2}{16} x(t_i)^3 + \cdots \right\} \mathbf{e}_\perp(t_i) \,, \tag{14}$$

where $\mathbf{e}_\perp(t_i)$ is the unit vector pointing to the Closest Axial Pont (CAP) on the cylinder axis from Earth at t_i. For detailed definitions of the fractional density depression and gradient, readers can refer to Kuwabara *et al.*[5] Note that $\mathbf{g}_\perp^{\rm exp}(t_i)$ is independent of the parameter a_0 denoting the magnitude of $I^{\rm exp}(t_i)$. We can calculate $x(t_i)$ and $\mathbf{e}_\perp(t_i)$ in (13) and (14), as follows.

The position vector of the CAP as viewed from Earth, $\mathbf{P}_E(t_i)$, is given by

$$\mathbf{P}_E(t_i) = \{\bar{\mathbf{V}}_{SW} - (\mathbf{e}_{\rm axis} \cdot \bar{\mathbf{V}}_{SW})\mathbf{e}_{\rm axis}\}(t_i - t_c) + \mathbf{P}_c\,, \tag{15}$$

where $\bar{\mathbf{V}}_{SW}$ is the average radial solar wind velocity, $\mathbf{e}_{\rm axis}$ is the unit vector parallel to the axis derived from the MFR analysis[5] and $\mathbf{P}_c$ is the CAP position at $t = t_c$. $\mathbf{P}_c$ is calculated from the impact time (t_d) and location ($\mathbf{d}$) of the MFR, as

$$\mathbf{P}_c = \mathbf{d} + \bar{\mathbf{V}}_{SW}(t_d - t_c)\,. \tag{16}$$

With $\mathbf{P}_E(t_i)$ in (15) and $R(t)$ in (4), we get $x(t_i)$ and $\mathbf{e}_\perp(t_i)$, as

$$x(t_i) = \frac{|\mathbf{P}_E(t_i)|}{R(t)}\,, \tag{17}$$

$$\mathbf{e}_\perp(t_i) = \frac{\mathbf{P}_E(t_i)}{|\mathbf{P}_E(t_i)|}\,. \tag{18}$$

We repeat the calculations for the expected density and gradient vector by introducing (17) and (18) into (13) and (14) for various values of κ_0, and find the best-fit κ_0 minimizing the residual S defined, as

$$S = \sqrt{\frac{1}{4N}\sum_{i=1}^{N}\{|I^{\rm obs}(t_i) - I^{\rm exp}(t_i)|^2 + |\mathbf{g}_\perp^{\rm obs}(t_i) - \mathbf{g}_\perp^{\rm exp}(t_i)|^2\}}\,. \tag{19}$$

Note that the best-fit value of a_0 for each κ_0 is uniquely given from the least-squares requirement, $\partial S^2/\partial a_0 = 0$, as

$$a_0 = \frac{\sum_{i=1}^{N} I^{\rm obs}(t_i)\frac{\partial I^{\rm exp}(t_i)}{\partial a_0}}{\sum_{i=1}^{N}\left(\frac{\partial I^{\rm exp}(t_i)}{\partial a_0}\right)^2}\,. \tag{20}$$

We perform the best-fitting calculation described above using the MFR parameters listed in Table 1, which were derived from our analysis of the

Table 1. MFR parameters used for the best-fit calculation for Halloween ICME event. These parameters were derived from *in situ* IMF observations using an expanding MFR model.[5,6]

MFR period	302.47–303.09 doy
Time of the first encounter with MFR (t_c)	302.47 doy
Radius of MFR at t_c(R_c)	0.174 AU
Time of the impact with MFR (t_d)	302.679 doy
Location of MFR at the impact (d_x, d_y, d_z) (AU)*	(0.000, −0.077, 0.060) AU
Latitude and longitude of the MFR axis direction (θ, ϕ)*	(46°, 54°)
Average solar wind velocity ($\bar{V}_{SW}$)	1323 km/s
Expansion velocity of MFR (V_c)	0.209 AU/day

*Values in the GSE coordinate system.

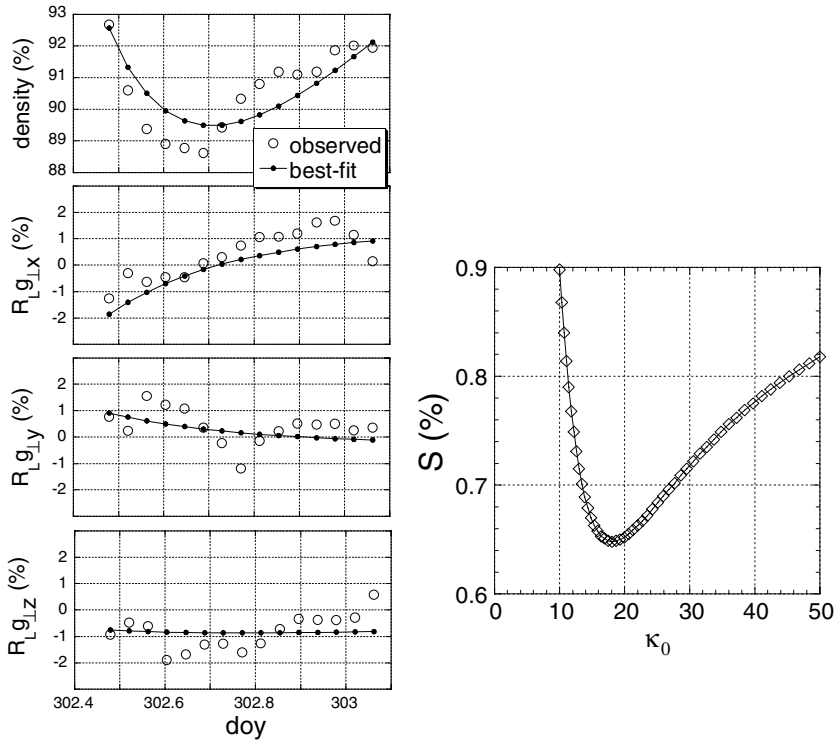

Fig. 3. Best-fitting model to the Halloween ICME event. Left panels show the density and three GSE components of the gradient vector, each as a function of time in the day of year (doy) in 2003. Open circles display the observed data, while the full circles connected by a line show the model best-fit to the data (see text). Right panel shows the mean residual of the best-fitting as a function of κ_0. The minimum residual ($S = 0.65\%$) is found at $\kappa_0 = 18$.

in situ IMF observations of the Halloween MFR.[6] The best-fit $I^{\rm exp}(t_i)$ and $\mathbf{g}_\perp^{\rm exp}(t_i)$ are compared with the observed data in Fig. 3. In this figure, we multiplied $\mathbf{g}_\perp^{\rm exp}(t_i)$ by the effective particle's gyroradius ($R_L = 0.044\,{\rm AU}$) derived from the CR cylinder analysis of the Halloween event for the direct comparison with the gradient vector deduced from the observed CR anisotropy.[6] It is seen in this figure that a reasonable agreement between the observed and modeled values is achieved even with such a simple model. Figure 3 also displays S as a function of the parameter κ_0 and indicates that the best-fit is achieved with $\kappa_0 = 18$ ($a_0 = -12\%$) and $S = 0.65\%$. The actual value of $\kappa_\perp$ at $t = t_c$ can be deduced from (4) and (5) with V_c

and R_c in Table 1, as

$$\kappa_\perp = \kappa_0 V_c R_c = 1.7 \times 10^{21}\,\mathrm{cm}^2/\mathrm{s}\,. \tag{21}$$

4. Summary and Conclusion

We developed a model of the cross-field diffusion of galactic CRs into an ICME based on the assumption that the local part of the ICME is an expanding straight cylinder. It is found that the spatial distribution (as a function of the normalized radial distance from the cylinder axis) of CR density in the rope rapidly reaches an equilibrium due to the balance between inward diffusion and adiabatic cooling in the expanding cylinder. This implies that the distribution is already stationary when the ICME arrives at Earth. By best-fitting the model distribution to the data observed by the muon detector network during the Halloween ICME/MFR event, the magnitude of the cross-field diffusion coefficient is evaluated to be $\kappa_\perp = 1.7 \times 10^{21}\,\mathrm{cm}^2/\mathrm{s}$. According to analyses of the diurnal anisotropy observed by muon detectors, the long-term average of the parallel mean free path of CRs is $\sim 2.0\,\mathrm{AU}$.[8,9] This implies

$$\kappa_{//} = \frac{1}{3\lambda_{//} c} \sim 3 \times 10^{23}\,\mathrm{cm}^2/\mathrm{s} \quad \text{and} \quad \frac{\kappa_\perp}{\kappa_{//}} \sim 0.0057 \tag{22}$$

for CRs with the median energy of $\sim 50\,\mathrm{GeV}$, to which surface muon detectors have major responses. This value of $\kappa_\perp/\kappa_{//}$ is consistent with theoretical expectations for the pitch angle scattering of CRs in the turbulent magnetic field in interplanetary space.[10] Note that the mean free path in MFR is likely to be longer than average, due to the exceptionally strong and smooth magnetic fields. Thus, the value in (22) might be regarded as an upper limit.

Acknowledgments

This work is supported in part by US NSF Grant ATM-0207196, and in part by Scientific Research (JSPS) in Japan and by the joint research program of the Solar-Terrestrial Environment Laboratory, Nagoya University.

References

1. H. V. Cane, *Space Sci. Rev.* **93** (2000) 55.
2. J. W. Bieber and P. Evenson, *Geophys. Res. Lett.* **25** (1998) 2955.

3. C. J. Farrugia *et al.*, *J. Geophys. Res.* **98** (1993) 7621.
4. M. Y. Hofer and E. O. Flückiger, *J. Geophys. Res.* **105** (2000) 23085.
5. T. Kuwabara *et al.*, *Geophys. Res. Lett.* **31** (2004) L19803-1.
6. T. Kuwabara, Ph.D. thesis, Shinshu University (2005) (in Japanese).
7. H. V. Cane, I. G. Richardson and G. Wibberenz, *Proc. 24th International Cosmic Ray Conference* **4** (1995) 377.
8. K. Munakata *et al.*, *Proc. 25th International Cosmic Ray Conference* **2** (1997) 77.
9. K. Munakata *et al.*, *Adv. Space Res.* **29** (2002) 1527.
10. J. W. Bieber, W. H. Matthaeus and A. Shalchi, *Geophys. Res. Lett.* **31** (2004) L10805-1.